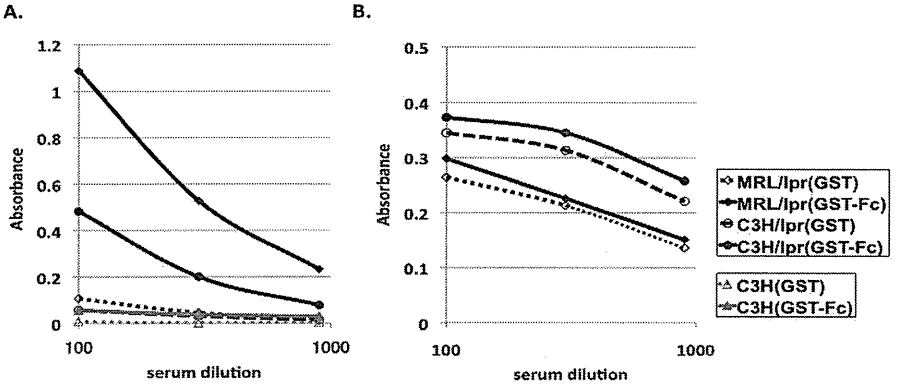

Fig. 4. RF activity of the mouse sera. The mouse sera from male mice of an arthritis-prone stain of mice, MRL/lpr and non-arthritic strain of mice, C3H/lpr (pooled sera at 16-20 weeks old, $n = 5$ each) were compared in a serial dilution. A. The capture ELISA plates, showed the sera from MRL/lpr mice was greater than those from C3H/lpr mice. The normal control sera from C3H/HeJ mice (pooled sera at 8 weeks old, $n = 12$) showed no reactivity. B. The same samples were measured on commercialized GST-ELISA plates. The results showed higher background, thus indicating the reaction to be non-specific for IgG-Fc. Absorbance indicates the mean value of OD_{405}-OD_{510} in triplicate samples.

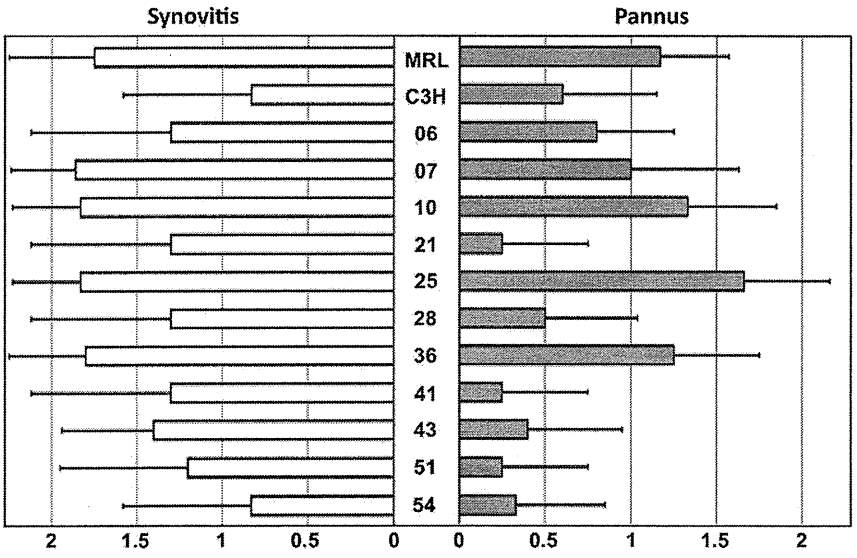

Fig. 5. Genetic dissociation of arthritis among the recombinant inbred strains MXH/lpr. The severity of arthritis of individual mice was graded at 16-20 weeks old ($n = 4$-6 each) and the results were represented as the average total score +/– S.D. of each strain (see Materials and Methods).

and 54 showed a lower score in the both severity. In addition, the severity between synovitis and pannus formation was highly correlated ($r = 0.725$, Fig. 7A), indicating that both lesions are on the same pathological sequence leading arthritis.

Then, the IgM- and IgG-RF activity of each stain of MXH/lpr mice was measured. As shown in Fig. 6, it was clearly demonstrated that IgM- and IgG-RF activity was also genetically dissociated among the MXH/lpr mice. IgG-RF activity of the line 41 was extremely higher than even the arthritis-prone parental strain of mice MRL/lpr ($p < 0.01$) and IgM-RF activity of the lines 06 and 36 was also higher than that of both parental strains ($p < 0.01$). There was only a slight negative correlation between both activities ($r = -0.286$, Fig. 7B).

Finally, correlation between the severity of arthritis and RF activity was examined. There was only a slight positive correlation between any two parameters; IgM-RF or IgG-RF vs. synovitis or pannus formation ($r < 0.265$ in any combinations, Fig. 7C and D).

Discussion

This study presented a novel method combining the GST-capture ELISA and the wheat germ cell-free protein

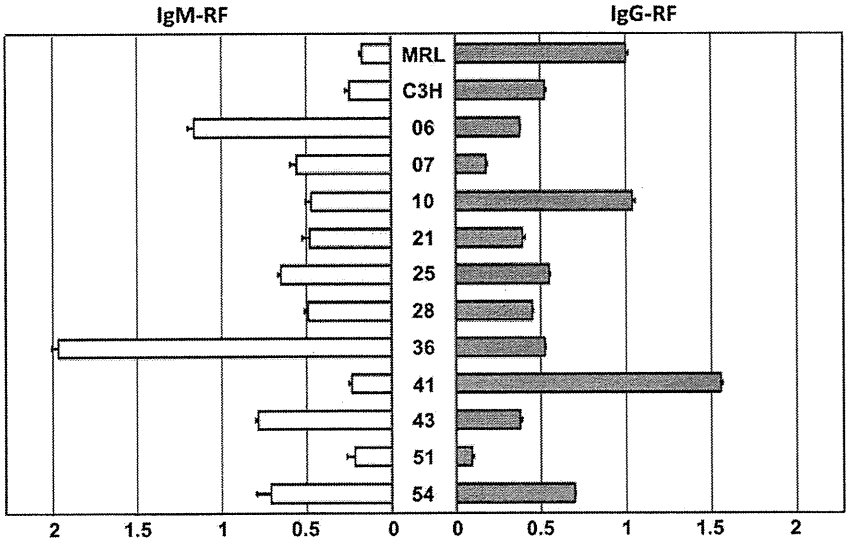

Fig. 6. Genetic dissociation of the RF activity among the recombinant inbred strains MXH/lpr. Mouse sera from each strain of male MXH/lpr mice were pooled at 16-20 weeks old, and they were reacted on the capture ELISA plates following a 100 × dilution. The results were represented as the average total score +/– S.D. in triplicate samples. Each of the studies was repeated three times and the similar results were obtained in all experiments.

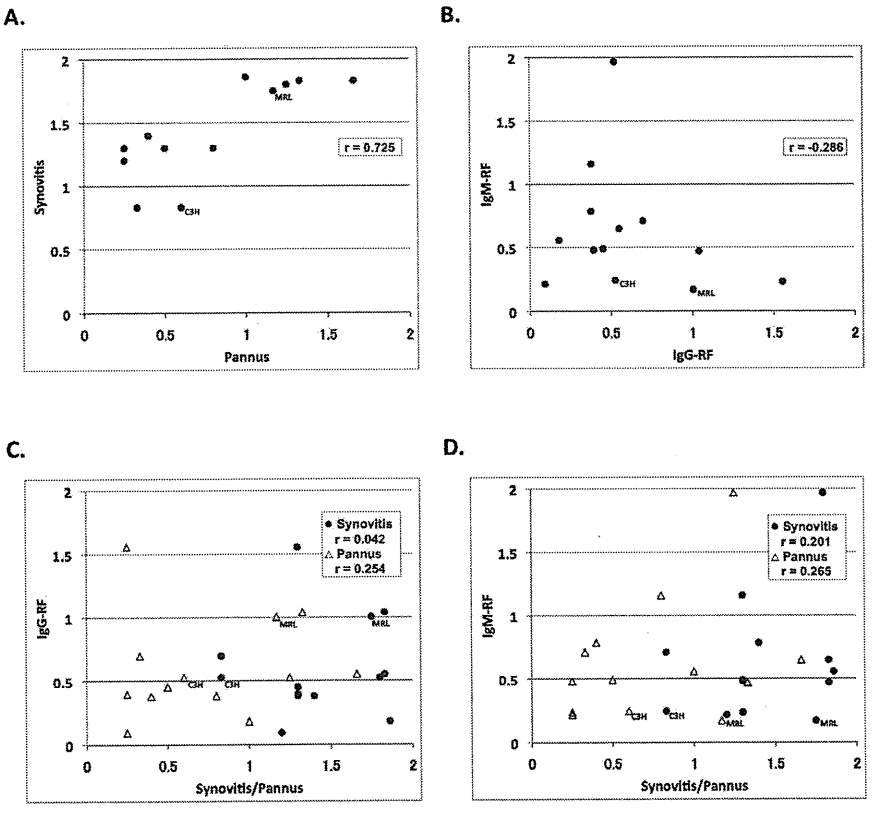

Fig. 7. Correlations of the severity of arthritis and RF activity. A correlation between any two parameters of the severity of arthritis and RF activity was estimated with the Spearman rank-correlation coefficient as indicated by *r*. A; synoviti vs. pannus, B; IgG-RF vs. IgM-RF, C; IgG-RF vs. synovitis/pannus and D; IgM-RF vs. synovitis/pannus.

production system, which thus provides high-throughput screening to clarify disease-specific autoantibodies in autoimmune diseases. The key points of this system are, first, to be able to use any kind of recombinant proteins fused to GST synthesized in the cell-free system without any purification processes, and second, to immobilize them on ELISA plates pre-coated with glutathione casein in one-step and at once.

This system was used to actually measure RF reacting with recombinant IgG-Fc with GST synthesized in the cell-free system. First, the RF specificity of this system was compared with a conventional ELISA containing *E. coli*-generated IgG-Fc using two types of monoclonal IgM-RF with a higher affinity and lower affinity. The results were similar between the two systems (Fig. 3). Next, the IgG-RF activity in mouse sera derived from MRL/lpr and C3H/lpr mice, which has higher RF activity in the former and lower in the later (Theofilopoulos and Dixon 1985), was measured, and compared their specificity with commercialized glutathione-coated ELISA plates. The results showed that the commercialized ELISA showed not only increased background but also absence of specific reactivity (Fig. 4B).

Then, this method was used to clearly demonstrate the genetic dissociation of RF from arthritis in a mouse model for RA. RI strains of mice MXH/lpr mice were prepared using two different parental inbred strains as progenitors, MRL/lpr and C3H/lpr mice, followed by an F1 intercross and more than 20 generations of strict brother-sister mating. This breeding protocol allows the production of a family of new inbred strains with special properties relative to each other since the genome of each RI strain consists of a random combination of genomes. MXH/lpr mice are the first RI strains in autoimmune disease model mice. In this study, the severity of arthritis was different among the strains, thus indicating that genome recombination between the parental strains regulates the severity of arthritis (Fig. 5). A previous study (Kamogawa et al. 2002) suggested that arthritis in MRL/lpr mice is under the control of multiple gene loci with an allelic combination derived from the original inbred strains by chromosomal mapping of the susceptibility loci to arthritis by using the backcross progeny of MRL/lpr × (MRL/lpr × C3H/lpr) F1 mice. The present results verified this proposed concept more clearly by using RI strains on the ground of the reason as described below.

In general, the genetic analysis of disease phenotypes by crossing disease-prone and non-disease prone strains allows for the examination of only the phenotype of one individual in an association with genotypes. This may make it difficult to analyze complex disease phenotypes in a reproducible fashion (Theofilopoulos et al. 1989). In this respect, a set of inbred strains having a genomic mosaic of progenitor strains such as MXH/lpr is considered to be a highly appropriate tool for analyzing the disease phenotypes in a reproducible fashion. In fact, the current study demonstrated genetic dissociation of the severity of arthritis and the RF activity (Figs. 6 and 7). RF has been considered as the argument that RA is an autoimmune disease, and also as the disease-specific autoantibodies in RA. However, the specificity and sensitivity of RF to RA are still controversial and a pathological basis of RA negative for RF, so called sero-negative RA, remains unclear. Our results may indicate that RF activity is not associated with the development of arthritis at least in this mouse model, and other autoantibodies, if present, could be considered as pathogenic autoantibodies.

Not only arthritis, but also other pathological phenotypes might be genetically segregated from autoantibodies, which have been reported as disease-specific antibodies. Therefore, the system using the capture ELISA with many synthetic proteins in cell free system may thus make it possible to perform a screening study of the protein reactants of autoantibodies and verify their significance for disease phenotypes in mouse models and also humans.

Acknowledgments

This work was supported by Research Funds from the Ministry of Health and Welfare of Japan and the Grant-in Aid for Scientific Research (B) of the Ministry of Education, Science and Culture of Japan (#18390123).

References

Endo, Y. & Sawasaki, T. (2006) Cell-free expression systems for eukaryotic protein production. *Curr. Opin. Biotech.*, **17**, 373-380.

Gawryl, M.S., Simon, M.T., Eatman, J.L. & Lint, T.F. (1986) An enzyme-linked immunoabsorbent assay for the quantitation of the terminal complement complex from cell membranes or in activated human sera. *J. Immunol. Methods*, **95**, 217-225.

Goshima, N., Kawamura, Y., Fukumoto, A., Miura, A., Honma, R., Satoh, R., Wakamatsu, A., Yamamoto, J., Kimura, K., Nishikawa, T., Andoh, T., Iida, Y., Ishikawa, K., Ito, E., Kagawa, N., Kaminaga, C., Kanehori, K., Kawakami, B., Kenmochi, K., Kimura, R., Kobayashi, M., Kuroita, T., Kuwayama, H., Maruyama, Y., Matsuo, K., Minami, K., Mitsubori, M., Mori, M., Morishita, R., Murase, A., Nishikawa, A., Nishikawa, S., Okamoto, T., Sakagami, N., Sakamoto, Y., Sasaki, Y., Seki, T., Sono, S., Sugiyama, A., Sumiya, T., Takayama, T., Takayama, Y., Takeda, H., Togashi, T., Yahata, K., Yamada, H., Yanagisawa, Y., Endo, Y., Imamoto, F., Kisu, Y., Tanaka, S., Isogai, T., Imai, J., Watanabe, S. & Nomura, N. (2008) Human protein factory for converting the transcriptome into an in vitro–expressed proteome. *Nat. Methods*, **5**, 1011-1017.

Kamogawa, J., Terada, M., Mizuki, S., Nishihara, M., Yamamoto, H., Mori, S., Abe, Y., Morimoto, K., Nakatsuru, S., Nakamura, Y. & Nose, M. (2002) Arthritis in MRL/lpr mice is under the control of multiple gene loci with an allelic combination derived from the original inbred strains. *Arthritis Rheum.*, **46**, 1067-1074.

Kitai, K., Kudo, T., Nakamura, S., Masegi, T., Ichikawa, Y. & Horikoshi, K. (1988) Extracellular production of human immunoglobulin G Fc region (hIgG-Fc) by *Escherichia coli*. *Appl. Microbiol. Biotechnol.*, **28**, 52-59.

Madin, K., Sawasaki, T., Ogasawara, T. & Endo, Y. (2000) A highly efficient and robust cell-free protein synthesis system prepared from wheat embryos: plants apparently contain a suicide system directed at ribosomes. *Proc. Natl. Acad. Sci. USA*, **97**, 559-564.

Moore, T.L., Dorner, R.W. & Zuckner, J.J. (1986) 19S IgM rheu-

matoid factor-7S IgG rheumatoid factor immune complexes isolated in patients with rheumatoid arthritis. *J. Lab. Clin. Med.*, **107**, 465-470.

Murphy, E.D. & Roths, J.B. (1978) Autoimmunity and lymphoproliferation: induction by mutant gene lpr, and acceleration by a male-associated factor in strain BXSB mice. In Rose, N.R., Bigazzai, P.E. & Warner, N.L., editors. Genetic control of autoimmune disease. *New York: Elsevier North Holland*, 207-220.

Nagata, S. (1994) Fas and Fas ligand: a death factor and its receptor. *Adv. Immunol.*, **57**, 129-144.

Nose, M., Nishimura, M., Ito, M.R., Itoh, J., Shibata, T. & Sugisaki, T. (1996) Arteritis in a novel congenic strain of mice derived from MRL/lpr lupus mice: Genetic dissociation from glomerulonephritis and limited autoantibody production. *Am. J. Pathol.*, **149**, 1763-1769.

Nose, M., Nishimura, M. & Kyogoku, M. (1989) Analysis of granulomatous arteritis in MRL/Mp autoimmune disease mice bearing lymphoproliferative genes. The use of mouse genetics to dissociate the development of arteritis and glomerulonephritis. *Am. J. Pathol.*, **135**, 271-280.

Nose, M., Takano, R., Nakamura, S., Arata, Y. & Kyogoku, M. (1990) Recombinant Fc of human IgG1 prepared in an Escherichia coli system escapes recognition by macrophages. *Int. Immunol.*, **2**, 1109-1112.

Nose, M. & Wigzell, H. (1983) Biological significance of carbohydrate chains on monoclonal antibodies. *Proc. Natl. Acad. Sci. USA*, **80**, 6632-6636.

Sawasaki, T., Hasegawa, Y., Tsuchimochi, M., Kamura, N., Ogasawara, T., Kuroita, T. & Endo, Y. (2002a) A bilayer cell-free protein synthesis system for high-throughput screening of gene products. *FEBS Lett.*, **514**, 102-105.

Sawasaki, T., Ogasawara, T., Morishita, R. & Endo, Y. (2002b) A cell-free protein synthesis system for high-throughput proteomics. *Proc. Natl. Acad. Sci. USA*, **99**, 14652-14657.

Sehr, P., Zumbach, K. & Pawlita, M. (2001) A generic capture ELISA for recombinant proteins fused to glutathione S-transferase: Validation for HPV serology. *J. immunol. Methods*, **253**, 153-162.

Soga, Y., Komori, H., Miyazaki, T., Arita, N., Terada, M., Kamada, K., Tanaka, Y., Fujino, T., Hiasa, Y., Matsuura, B., Onji, M. & Nose, M. (2009) Toll-like receptor 3 signaling induces chronic pancreatitis through the Fas/Fas ligand-mediated cytotoxicity. *Tohoku J. Exp. Med.*, **217**, 175-184.

Takahashi, S., Itoh, J., Nose, M., Ono, M., Yamamoto, T. & Kyogoku, M. (1993) Cloning and cDNA sequence analysis of nephritogenic monoclonal antibodies derived from an MRL/lpr lupus mouse. *Mol. Immunol.*, **30**, 177-182.

Takai, K., Sawasaki, T. & Endo, Y. (2010) Practical cell-free protein synthesis system using purified wheat embryos. *Nat. Protoc.*, **5**, 227-238.

Tan, E.M. (1989) Antinuclear antibodies: diagnostic markers for autoimmune diseases and probes for cell biology. *Adv Immunol.*, **44**, 93-151.

Theofilopoulos, A.N. & Dixon, F.J. (1985) Murine models of systemic lupus erythematosus. *Adv. Immunol.*, **37**, 269-390.

Theofilopoulos, A.N., Kofler, R., Singer, P.A. & Dixon, F.J. (1989) Molecular genetics of murine lupus models. *Adv. Immunol.*, **46**, 61-109.

Valdés Veliz, R., García, J., Reyes, B., Muñoz, L., Alvarez, T., Padilla, S., Abrahantes Mdel, C., Zubiaurrez, J., Agraz, A. & Marrero, A. (2003) A very sensitive enzyme-linked immunoabsorbent assay to Staphylococcal protein A in the presence of immunoglobulins. *Biochem. Biophys. Res. Commun.*, **303**, 863-867.

Chapter 13

Cell-Free Protein Synthesis for Structure Determination by X-ray Crystallography

Miki Watanabe, Ken-ichi Miyazono, Masaru Tanokura, Tatsuya Sawasaki, Yaeta Endo, and Ichizo Kobayashi

Abstract

Structure determination has been difficult for those proteins that are toxic to the cells and cannot be prepared in a large amount in vivo. These proteins, even when biologically very interesting, tend to be left uncharacterized in the structural genomics projects. Their cell-free synthesis can bypass the toxicity problem. Among the various cell-free systems, the wheat-germ-based system is of special interest due to the following points: (1) Because the gene is placed under a plant translational signal, its toxic expression in a bacterial host is reduced. (2) It has only little codon preference and, especially, little discrimination between methionine and selenomethionine (SeMet), which allows easy preparation of selenomethionylated proteins for crystal structure determination by SAD and MAD methods. (3) Translation is uncoupled from transcription, so that the toxicity of the translation product on DNA and its transcription, if any, can be bypassed. We have shown that the wheat-germ-based cell-free protein synthesis is useful for X-ray crystallography of one of the 4-bp cutter restriction enzymes, which are expected to be very toxic to all forms of cells retaining the genome. Our report on its structure represents the first report of structure determination by X-ray crystallography using protein overexpressed with the wheat-germ-based cell-free protein expression system. This will be a method of choice for cytotoxic proteins when its cost is not a problem. Its use will become popular when the crystal structure determination technology has evolved to require only a tiny amount of protein.

Key words: Structural genomics, Toxic protein, Wheat germ, Restriction enzyme, Selenomethionine, SAD

1. Introduction

In general, it is difficult to determine crystal structure of proteins toxic to cells because the toxicity does not allow their preparation in a large amount for crystallization. Many of those cytotoxic proteins may play important biological roles, but their structural diversity may be left unexplored, especially in the context of the

Y. Endo et al. (eds.), *Cell-Free Protein Production: Methods and Protocols*, Methods in Molecular Biology, vol. 607
DOI 10.1007/978-1-60327-331-2_13, © Humana Press, a part of Springer Science+Business Media, LLC 2010

structural genomics. In addition to novel structural folds that expand the universe of protein structure, elucidation of their structure may reveal novel modes of protein–DNA interaction and protein–protein interaction among others (1, 2).

Restriction endonucleases, essential tools for molecular biology, form a good example of such groups of cytotoxic proteins with important biological roles and structural diversity (3–5). A restriction endonuclease recognizes a specific DNA sequence and introduces a double-stranded break, while a paired modification enzyme can methylate a specific base of the same sequence. Their genes are usually tightly linked and form a restriction–modification gene complex. Various lines of evidence indicate that they behave as selfish mobile genetic elements just as viral genomes and transposons. Comparison of two closely-related genome sequences, such as those of two species within the same hyperthermophilic archaeon genus, *Pyrococcus abyssi* and *Pyrococcus horikoshii*, has indicated their mobility and linkage with various types of genome rearrangements (6). This property makes it possible to search restriction enzymes of a novel fold by bioinformatics methods. While the restriction endonucleases show little sequence conservation, the methyltransferases belong to a conserved protein family. Therefore, the bioinformatics strategy is to first identify methyltransferase genes and then search for their cognate restriction endonuclease genes in the neighboring open reading frames (ORFs) (7). If genome comparison reveals that the candidate gene has been moving between genomes together with the methyltransferase homolog, it is likely a restriction gene. This strategy allowed identification of PabI from *P. abyssi* as a unique 4-bp cutter restriction enzyme with novel properties, generation of TA3′ restriction terminus, and Mg^{2+} ion independence (7, 8).

PabI was predicted to adopt an entirely novel structure (7). However, PabI, like most of the restriction enzymes, is cytotoxic when expressed in vivo in the absence of appropriate and sufficient methylation on the genome. The strategies to bypass this toxicity include use of tightly repressible expression systems and expression of the cognate methyltransferase, but they did not work well. In contrast, in vitro translation systems can synthesize almost any protein, often with high accuracy and at a speed approaching in vivo rates. Among the cell-free systems, the wheat-germ-based system is of special interest: the translation machine has little codon preference and, especially, has little discrimination between methionine (Met) and selenomethionine (SeMet), a characteristic that is useful in crystal structure determination by SAD and MAD methods; translation is uncoupled from transcription, so that digestion of the template DNA by the produced restriction enzyme does not take place (8). The only problem with the system is the cost, especially in a large scale.

In this chapter, we describe successful preparation of PabI protein in this wheat-germ-based cell-free expression system in the native and SeMet-labeled forms (Fig. 13.1), their crystallization (Fig. 13.2), and structure determination. The crystal structure, mutant analysis and *in silico* modeling revealed that the protein adopts a novel fold and participates in a novel mode of protein–DNA interaction (8). The new nomenclature and abbreviations for restriction enzymes and their genes were used (9).

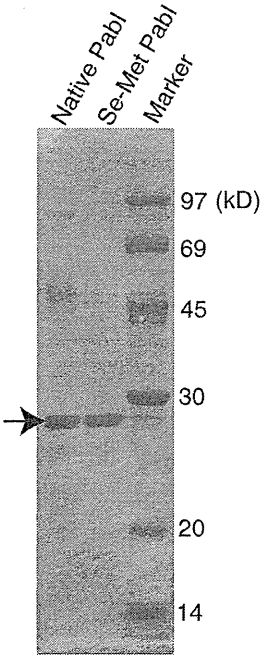

Fig 13.1 PabI restriction enzyme and its selenomethionine-substituted version expressed in a wheat-germ-based cell free expression system. SDS-PAGE.

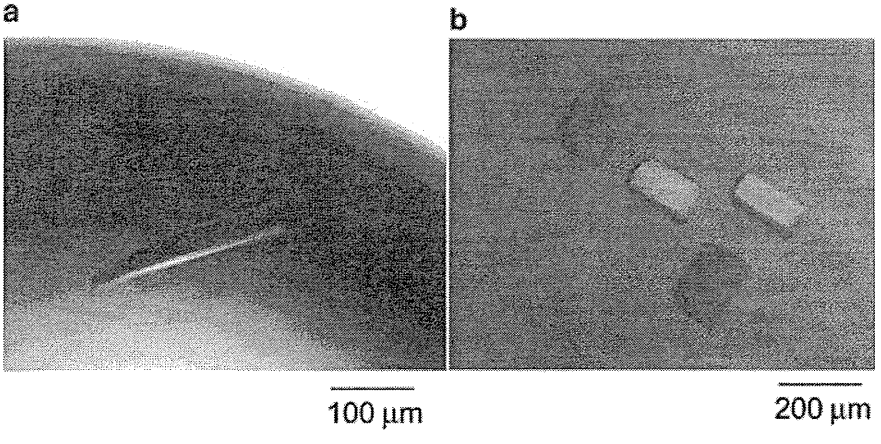

Fig 13.2. Crystals of PabI (**a**) and its seleomethionine-substituted version (**b**) prepared in a wheat-germ-based cell free expression system.

2. Materials

2.1. Production and Purification of the Native and Selenomethionine-Substituted Forms of the Protein

1. High-quality circular preparation of plasmid pEU-*pabIR*: the PabI gene (*pabIR*) is inserted into the multiple cloning site of pEU3b specialized for cell-free expression (10) prepared from *Escherichia coli* strain: JM109 {*recA1 endA1 gyrA96 thi hsdR17* (rK$^-$ mK$^+$) e14 (*mcrA*) *supE44 relA1* Δ(*lac-proAB*)/[F′ *traD36 proAB+ lacIq lacZ* ΔM15]} (11) (see Note 1).
2. Milli-Q water, freshly prepared.
3. 5× Transcription buffer (TB): 400 mM HEPES-KOH, pH 7.8, 80 mM magnesium acetate, 10 mM spermidine, and 50 mM DTT.
4. Nucleotide tri-phosphates (NTPs) mix: a solution containing 25 mM each of ATP, GTP, CTP, and UTP.
5. SP6 RNA polymerase (80 units/μL, Promega).
6. RNasin (80 units/μL, Promega).
7. Translational substrate buffer (TSB): 30 mM HEPES-KOH, pH 7.8, 100 mM potassium acetate, 2.7 mM magnesium acetate, 0.4 mM spermidine, 2.5 mM DTT, 0.3 mM amino acid mix (20 standard amino acids), 1.2 mM ATP, 0.25 mM GTP, and 16 mM creatine phosphate.
8. SeMet buffer: 30 mM HEPES-KOH, pH 7.8, 100 mM potassium acetate, 2.7 mM magnesium acetate, 0.4 mM spermidine, 2.5 mM DTT, 0.3 mM each of 20 standard amino acids except for methionine, 1.2 mM ATP, 0.25 mM GTP, 16 mM creatine phosphate, and 250 μM selenomethionine.
9. 6-Well plate (3.2 cm in diameter, Whatman Inc., Clifton, NJ).
10. Wheat embryo extract (240 OD/mL) or WEPRO®1240 (CellFree Sciences Co., Ltd.).
11. 20 mg/mL creatine kinase (Roche Diagnostics K. K.).
12. Sephadex G-25 (fine) column (Amersham Biosciences).
13. Heparin–sepharose purification buffer: 10 mM Tris–HCl pH7.5, 1 mM DTT, 0–2 M NaCl gradient.
14. ÄKTA purifier chromatography system (GE healthcare).
15. Protein storage buffer: 10 mM Tris–HCl (pH 7.5), 200 mM NaCl, and 1 mM DTT.

2.2. Crystallization and Structure Determination

1. INTELLI-PLATEs and CrysChem plates for crystallization were purchased from Art Robbins Instruments and Hampton research, respectively.

2. Crystal screen HT, Index HT, Grid screening PEG6000 for the first screening of the crystallization conditions were purchased from Hampton research.
3. Wizard I and II purchased from Emerald BioStructure were used for the first screening of the crystallization condition.
4. Computer programs: HKL2000 (12) for integration and scaling of X-ray diffraction data; SnB (13) for determination of the selenium substructure of the Se-Met variant; SHARP (14) for refinement of the selenium sites and calculation of the initial phase; RESOLVE (15) for automated initial model building and refinement; MOLREP (16) for molecular replacement; Refmac5 (17) and CNS (18) for refinement of the model; XtalView (19) for manual model building.

3. Methods

Cell-free translation of proteins can be achieved mainly by three different modes, batch mode translation (20, 21), bilayer system (22), and CFCF protein synthesis method (10, 23). In the cell-free protein production, mRNA purification represents the most time-consuming step. Recently, based on the bilayer system, a sequential transcription–translation method was developed by directly mixing a transcribed mixture and the wheat germ extract (24). This method provides a very simple system to scale up translational mixture for large-scale protein production because it directly uses unpurified transcriptional mixture without mRNA purification. We used the method for mass production of PabI protein with Met (native) or SeMet (SeMet-substituted) (Fig. 13.1). After purification, native and SeMet-substituted proteins were used for crystallization (Fig. 13.2) and structure determination by X-ray crystallography (8).

3.1. Production and Purification of the Native and SeMet-Substituted Forms of the Protein

3.1.1. mRNA Synthesis

1. Prepare, in a 15-ml tube, 150 µg of high-quality circular plasmid molecules as templates, 1.2 mL of 5× TB, 0.6 mL of 25 mM NTP mix, 70 µL of SP6 RNA polymerase, 70 µL of RNasin, and Milli-Q water (to 6 mL).
2. Incubate the 15-mL tube at 37°C for 4 h (termed "mRNA solution").

3.1.2. Synthesis of Native Protein

1. Prepare four plates each with 6 wells (24 wells in all) (see Note 2).
2. Add 5.5 ml of TSB to each well.
3. Resuspend the white pellet present in the mRNA solution (Subheading 3.1.1) by gently mixing up and down without bubbling.

4. Prepare the translation mixture: 6 mL of the above mRNA solution, 6 mL of wheat-germ extract, and 24 µL of 20 mg/mL creatine kinase.
5. Mix carefully the translational mixture without bubbling.
6. Transfer carefully 500 µL of the translational mixture into the bottom of each well containing the substrate mixture.
7. Incubate the four plates at 26°C for 16 h (see Note 3).

3.1.3. Preparation of SeMet-Substituted Wheat Germ Extract

1. Gel-filtrate 6 mL of the wheat germ extract through 25-mL Sephadex G-25 (fine) column, equilibrated with 50 mL of SeMet buffer.
2. Collect the void fraction.
3. Store at –80°C until use.

3.1.4. Synthesis of SeMet-Substituted Protein

1. Prepare four plates (24 wells in all) (see Note 2).
2. Add 5.5 ml of SeMet buffer to each well.
3. Resuspend the white pellet present in the mRNA solution (Subheading 3.1.1) by gently mixing up and down without bubbling.
4. Prepare SeMet-substituted translation mixture: 6 mL of the above mRNA solution, 6 mL of the SeMet-substituted wheat-germ extract (Subheading 3.1.3), and 24 µL of 20 mg/mL creatine kinase.
5. Mix carefully the SeMet-substituted translational mixture without bubbling.
6. Transfer carefully 500 µL of the SeMet-substituted translational mixture into the bottom of each well containing the SeMet buffer.
7. Incubate the four plates at 26°C for 16 h (see Note 3).

3.1.5. Purification of the Synthesized PabI Protein (a Heat-Resistant Protein)

1. Heat the translational mixture at 90°C for 15 min.
2. Remove the denatured proteins and insoluble materials by centrifugation (10,000×*g*; 15 min; 4°C).
3. Purify PabI protein in the supernatant by a Heparin–Sepharose affinity column using ÄKTA purifier chromatography system.
4. Store the purified PabI protein in protein storage buffer at 4°C.

3.2. Crystallization and Structure Determination

In this section, we describe our experience with one protein in the indicative mood instead of the imperative mood.

3.2.1. Crystallization

1. The crystallization of PabI was performed by the sitting drop vapor diffusion method using the INTELI-PLATE (for initial screening of 96 conditions) and the CrysChem plate (for crystallization screening of 24 conditions).

2. Initial screening of crystallization condition was performed by the sparse-matrix screening method using commercially available screening kits of Crystal screen HT (96 conditions), Index HT (96 conditions), Grid screening PEG6000 (24 conditions), and Wizard I and II (96 conditions). Each crystallization drop was made by mixing 1 μL of the protein solution [0.5 mg/mL protein in 10 mM Tris-HCl (pH 7.5), 200 mM NaCl, and 1 mM dithiothreitol (DTT)] and an equal volume of the reservoir solution.
3. Because of the low solubility of PabI, we used a low concentration solution (0.5 mg/ml) for the first screening. Though the concentration of protein solution was quite low, crystals of PabI could be obtained in the reservoir solution containing PEG6000 as precipitant. The best crystal of PabI appeared under the reservoir conditions containing 100 mM MES (pH 6.0) and 5% PEG6000 after 2 weeks. Typical size of these crystals was $50 \times 50 \times 200$ μm.
4. Although crystals of the Se-Met variant of PabI were also obtained under identical protein solution condition and reservoir solution condition, their size and quality were worse than those of the native crystals. For the improvement of crystal quality, the protein solution condition was modified to increase the solubility of the Se-Met variant. Se-Met variant of PabI was dialyzed against 10 mM MES (pH 6.0), 200 mM NaCl, 10 mM $MgCl_2$, and 10 mM DTT and concentrated to 1.9 mg/ml. The best crystal of the Se-Met variant of PabI was grown under the reservoir conditions containing 50 mM MES (pH 6.8) and 1% PEG6000 using the concentrated protein solution after 1 day.

3.2.2. Structure Determination

1. The X-ray diffraction datasets of the crystals of native PabI and its Se-Met variant were collected using high-brilliance X-ray generated by synchrotron radiation in Photon Factory (Tsukuba, Japan).
2. All the measurements were carried out under cryogenic conditions to reduce radiation damage. Each crystal was soaked in a corresponding reservoir solution containing 20% ethylene glycerol (final concentration) as the cryoprotectant, before being picked up and flash-cooled in a dry nitrogen stream at 95 K.
3. The diffraction data of the native crystal were collected at a wavelength of 1.000Å using a Quantum 315 CCD detector (ADSC) at the BL-5A beamline in Photon factory. A native crystal of PabI diffracted X-rays to a resolution of 3.0Å. The X-ray diffraction data were integrated and scaled with the program HKL2000 (23). Analysis of the diffraction date showed that the native PabI crystal belonged to the primitive monoclinic space group $P2_1$ with the unit cell parameters of a= 84.6Å, b=114.0 Å, c=89.2Å, and β=116.3°. Data collection, phasing, and refinement statistics of PabI are summarized in Table 13.1.

Table 13.1
Data collection, phasing, and refinement statistics of R.PabI

	Native crystal	Se-Met labeled crystal
Data collection		
Beamline	Photon Factory BL-5A	Photon Factory NW12
Detector	ADSC Quantum 315	ADSC Quantum 210r
Data collection temperature (K)	95	95
Wave length (Å)	1.0000	0.9792
Unit Cell dimensions *a*, *b*, *c* (Å) β (degree)	84.6, 114.0, 89.2 116.3	84.6, 114.5, 89.4 116.3
Space Group	$P2_1$	$P2_1$
Resolution (Å)	20–3.0 (3.11–3.00)	20–2.9 (3.00–2.90)
Completeness	99.3 (96.7)	100.0 (100.0)
Unique reflection	30687	33650
Averaged redundancy	3.6 (3.4)	7.5 (7.6)
R_{merge} (%)	6.7 (28.3)	7.7 (28.0)
I/sigma	14.8 (4.5)	17.8 (5.1)
Phasing		
R_{cullis}		0.748
Phasing power		1.27
FOM before density modification		0.31
FOM after density modification		0.86
Refinement		
Number of nonhydrogen atoms		
Protein	10,599	
Water	0	
R/R_{free} (%)	24.9/31.8	
RMSD bond length (Å)	0.009	
RMSD bond angle (deg.)	1.5	
Ramachandran plot		
In most favored regions (%)	74.0	
In additional allowed regions (%)	22.3	
In Generously allowed regions (%)	2.3	
In disallowed regions (%)	1.4	

Values in parentheses are for the highest resolution shell

4. To determine the structure of PabI, which was predicted to possess novel protein fold (7), we applied SAD (single-wavelength anomalous dispersion) phasing method using the Se-Met variant crystal. The diffraction data of Se-Met crystal were collected at a wavelength of 0.9792 Å using a Quantum 210r CCD detector (ADSC) at the NW12 beam line in Photon Factory. Diffraction data of the Se-Met variant of PabI were processed in the same way. Analysis of the diffraction date showed that a Se-Met variant crystal diffracted X-rays to a resolution of 2.9 Å and belonged to the same space group as the native crystal, $P2_1$ with the unit cell parameters of a=84.6 Å, b=114.2 Å, c=89.4 Å, and β=116.3°.
5. Consideration of the Matthew's coefficient (25) (V_M) suggests that native and Se-Met variant crystals of PabI have six protein molecules per asymmetric unit (V_M=2.5 Å^3/Da).
6. The crystal structure of PabI was determined by the SAD phasing method using the diffraction data set of the crystal of the Se-Met variant. The selenium substructure was determined by a direct method program, SnB (13). A total of 19 selenium sites was determined in the asymmetric unit. Because each PabI molecule possesses six methionine sites, this result indicated that approximately 80% of the selenium sites were detected by the SnB calculation.
7. Refinement of the coordinates of the selenium sites and calculation of the initial phase were performed using the program SHARP (14). Phase calculation resulted in an overall figure of merit (FOM) of 0.31 for the resolution range of 20–2.9 Å. After that, density modification and initial model building were performed with the program RESOLVE (15). Molecular models of 759 residues (56% of the total) were automatically built with this calculation.
8. The initial model of the Se-Met variant of PabI was refined and manually rebuilt with the programs CNS (18) and XtalView (19), using 10% (randomly chosen) of the reflections to calculate the R_{free}. The partially built protomer model was transformed into the other five subunits using the program MOLREP (16) in CCP4 (26) and refined with the program REFMAC5 (17) with noncrystallographic symmetry (NCS) restraints.
9. Crystal structure of the native PabI was determined by a molecular replacement method using the coordinates of the partially built structure of the Se-Met variant crystal with the program MOLREP (16). The final structure of PabI was refined and built using the diffraction data set (20–3.0 Å) of native crystal with the program CNS (without NCS restraints) and XtalView (see Note 4).
10. As a result, we were able to determine the structure of PabI at 3.0 Å resolution. The current model has been refined to an

R-factor and R_{free} values of 24.9% and 31.8%, respectively. The paper on the structure of PabI represents the first report of structure determination by X-ray crystallography using the protein overexpressed with the wheat-germ-based cell-free protein expression system (8).

4. Notes

1. RNase contamination is dramatically decreased by protein production in the cell-free system. Unfortunately, however, it is difficult to control the contamination even though commercially available kits are used. To prepare high-quality circular plasmid molecules, we use extraction with phenol/chloroform (phenol:chloroform:isoamyl alcohol = 24:24:1, pH 7.9) and with chloroform after plasmid purification by commercially available kits such as those by Qiagen.
2. To obtain a sufficient amount of PabI, we used four plates (24 wells in all). Twenty-four wells of the reaction gave approximately 3 mg of native and SeMet-substituted PabI.
3. For unstable proteins, incubation at 17°C for 18 h is better.
4. We did not use NCS refinement in the final step of refinement because R-factor and R_{free} values became worse when refined with NCS restraint. We could not build coordinates of water molecules and other nonprotein atoms in this structure.

Acknowledgments

The study of PabI was carried out in collaboration with Jan Kosinski, Ken Ishikawa, Masayuki Kamo, Koji Nagata, and Janusz M. Bujnicki. We are grateful to Kazuyuki Takai for encouragements and patience. IK was supported, during writing, by twenty-first century COE program "Genome and Language" from MEXT and "Grants-in-Aid for Scientific Research" (19657002, 21370001) from JSPS.

References

1. Zhang, Q. and Wang, Y. (2008) High mobility group proteins and their post-translational modifications. *Biochim. Biophys. Acta* **1784**, 1159–1166.
2. Hay, R.T. (2005) SUMO: a history of modification. *Mol. Cell* **18**, 1–12.
3. Kobayashi, I. (2001) Behavior of restriction-modification systems as selfish mobile elements and their impact on genome evolution. *Nucleic Acids Res.* **29**, 3742–3756.
4. Kobayashi, I. (2004) Restriction – modification systems as minimal forms of life. In

Restriction Endonucleases (Pingoud, A., ed.), Berlin, Springer. pp. 19–62.

5. Orlowski, J. and Bujnicki, J.M. (2008) Structural and evolutionary classification of Type II restriction enzymes based on theoretical and experimental analyses. *Nucleic Acids Res.* **36,** 3552–3569.
6. Chinen, A., Uchiyama, I. and Kobayashi, I. (2000) Comparison between Pyrococcus horikoshii and Pyrococcus abyssi genome sequences reveals linkage of restriction-modification genes with large genome polymorphisms. *Gene* **259,** 109–121.
7. Ishikawa, K., Watanabe, M., Kuroita, T., Uchiyama, I., Bujnicki, J.M., Kawakami, B., Tanokura, M. and Kobayashi, I. (2005) Discovery of a novel restriction endonuclease by genome comparison and application of a wheat-germ-based cell-free translation assay: PabI (5′-GTA/C) from the hyperthermophilic archaeon *Pyrococcus abyssi. Nucleic Acids Res.* **33,** e112.
8. Miyazono, K., Watanabe, M., Kosinski, J., Ishikawa, K., Kamo, M., Sawasaki, T., Nagata, K., Bujnicki, J.M., Endo, Y., Tanokura, M. and Kobayashi, I. (2007) Novel protein fold discovered in the PabI family of restriction enzymes. *Nucleic Acids Res.* **35,** 1908–1918.
9. Roberts, R.J., Belfort, M., Bestor, T., Bhagwat, A.S., Bickle, T.A., Bitinaite, J., Blumenthal, R.M., Degtyarev, S.Kh., Dryden, D.T., Dybvig, K., Firman, K., Gromova, E.S., Gumport, R.I., Halford, S.E., Hattman, S., Heitman, J., Hornby, D.P., Janulaitis, A., Jeltsch, A., Josephsen, J., Kiss, A., Klaenhammer, T.R., Kobayashi, I., Kong, H., Krüger, D.H., Lacks, S., Marinus, M.G., Miyahara, M., Morgan, R.D., Murray, N.E., Nagaraja, V., Piekarowicz, A., Pingoud, A., Raleigh, E., Rao, D.N., Reich, N., Repin, V.E., Selker, E.U., Shaw, P.C., Stein, D.C., Stoddard, B.L., Szybalski, W., Trautner, T.A., Van Etten, J.L., Vitor, J.M., Wilson, G.G. and Xu, S.Y. (2003) A nomenclature for restriction enzymes, DNA methyltransferases, homing endonucleases and their genes. *Nucleic Acids Res.* **31,** 1805–1812.
10. Sawasaki, T., Ogasawara, T, Morishita, R. and Endo, Y. (2002) A cell-free protein synthesis system for high-throughput proteomics. *Proc. Natl. Acad. Sci. U.S.A.* **99,** 14652–14657.
11. Yanisch-Perron, C., Vieira, J. and Messing, J. (1985) Improved M13 phage cloning vectors and host strains: nucleotide sequences of the M13mp18 and pUC19 vectors. *Gene* **33,** 103–119.
12. Otwinowski, Z. and Minor, W. (1997) Processing of X-ray diffraction data collected in oscillation mode. *Methods Enzymol.* **276,** 307-326.
13. Weeks, C. and Miller, R. (1999) The design and implementation of SnB version 2.0. *J. Appl. Cryst.* **32,** 120–124.
14. Bricogne, G., Vonrhein, C., Flensburg, C., Schiltz, M. and Paciorek, W. (2003) Generation, representation and flow of phase information in structure determination: recent developments in and around SHARP 2.0. *Acta Crystallogr. D Biol. Crystallogr.* **59,** 2023–2030.
15. Terwilliger, T. (2003) Automated main-chain model building by template matching and iterative fragment extension. *Acta Crystallogr. D Biol. Crystallogr.* **59,** 38–44.
16. Vagin, A. and Teplyakov, A. (1997) MOLREP: an automated program for molecular replacement. *J. Appl. Cryst.* **30,** 1022-1025.
17. Murshudov, G. N., Vagin, A. A. and Dodson, E. J. (1997) Refinement of macromolecular structures by the maximum-likelihood method. *Acta Crystallogr. D Biol. Crystallogr.* **53,** 240–255.
18. Brunger, A. T., Adams, P. D., Clore, G. M., DeLano, W. L., Gros, P., Grosse-Kunstleve, R. W., Jiang, J. S., Kuszewski, J., Nilges, M., Pannu, N. S., Read, R. J., Rice, L. M., Simonson, T. and Warren, G. L. (1998) Crystallography & NMR system: A new software suite for macromolecular structure determination. *Acta Crystallogr. D Biol. Crystallogr.* **54,** 905–921.
19. McRee, D. E. (1999) XtalView/Xfit – a versatile program for manipulating atomic coordinates and electron density. *J. Struct. Biol.* **125,** 156–165.
20. Madin, K., Sawasaki, T., Ogasawara, T. and Endo, Y. (2000) A highly efficient and robust cell-free protein synthesis system prepared from wheat embryos: plants apparently contain a suicide system directed at ribosomes. *Proc. Natl. Acad. Sci. U.S.A.* **97,** 559-564
21. Hanes, J. and Pluckthun, A. (1997) *In vitro* selection and evolution of functional proteins by using ribosome display. *Proc. Natl. Acad. Sci. U.S.A.* **94,** 4937–4942.
22. Sawasaki, T., Hasegawa, Y., Tsuchimochi, M., Kamura, N., Ogasawara, T. and Endo Y. (2002) A bilayer cell-free protein synthesis system for high-throughput screening of gene products. *FEBS Lett.* **514,** 102–105.
23. Spirin, A. S., Baranov, V. I., Ryabova, L. A., Ovodov, S. Y. and Alakhov, Y. B. (1988) A continuous cell-free translation system capable of producing polypeptides in high yield. *Science* **242,** 1162–1164.

24. Sawasaki, T., Gouda, M.D., Kawasaki, T., Tsuboi, T., Tozawa, Y., Takai, K. and Endo, Y. (2005) The wheat germ cell-free expression system: methods for high-throughput materialization of genetic information. *Methods Mol. Biol.* **310,** 131–144.

25. Matthews, B. W. (1968) Solvent content of protein crystals. *J. Mol. Biol.* **33,** 491–497.

26. Collaborative, Computational, Project, Number, 4. (1994) The CCP4 suite: programs for protein crystallography. *Acta Crystallogr. D Biol. Crystallogr.* **50,** 760–763.

Chapter 7

Cell-Free-Based Protein Microarray Technology Using Agarose/DNA Microplate

Tatsuya Sawasaki and Yaeta Endo

Abstract

Protein microarray is considered to be one of the key analytical tools for high-throughput protein function analysis. We found that Arabidopsis HY5 protein functions as a novel DNA-binding tag (DBtag), and DBtagged proteins are immobilized and purified on a newly designed agarose/DNA microplate. In this chapter, we demonstrate a protocol for making the DBtag-based protein microarray and will provide protocols for two applications using the microarray: (1) detection of autophosphorylation activity of DBtagged human protein kinases and inhibition of their activity by staurosporine, and (2) detection of a protein–protein interaction between the DBtagged UBE2N and UBE2v1.

Key words: Protein microarray, High-throughput functional analysis, DNA-binding tag, Protein kinase, Agarose/DNA microplate

1. Introduction

Currently available protein microarray technology has allowed large-scale screening of biomarker proteins recognized by serum antibodies (1). However, this method is yet to become a commonly used biochemical tool for the analysis of proteins (2). Certainly there is room for further improvement before this technology could become a routinely used laboratory tool. For example, one of the problems is the difficulty in immobilizing a variety of proteins in their functionally active forms. Many proteins needed to be appropriately oriented for proper functioning (3). However, it is not easy to control the orientation of the protein during its mobilization on the surface of the microplate. Another problem is that the high-throughput functional analysis requires freshly produced and purified proteins; however, unlike DNA, many purified proteins are not stable and thus, these cannot

Y. Endo et al. (eds.), *Cell-Free Protein Production: Methods and Protocols,* Methods in Molecular Biology, vol. 607
DOI 10.1007/978-1-60327-331-2_7,

be stored in active condition for long time. The development of functional protein microarrays for practical use, therefore, requires relatively easy methods for the functional immobilization and purification of freshly prepared proteins on the microplate. We recently developed a high-throughput method for protein synthesis using the wheat germ cell-free protein synthesis and an automatic protein synthesizer (4–6) and demonstrated that the automatic synthesizer is very useful for the production of freshly prepared proteins.

To create a new type of protein microarray, we developed a novel tag using a DNA-binding protein and a newly designed microplate consisting of agarose and commercially available genomic DNAs (7). The new tag, named here as DBtag, is the Arabidopsis transcription factor HY5 having a basic leucine-zipper domain (8). We found that the HY5 protein had high binding affinity to commercially available salmon sperm and calf DNAs. Here, we used this DNA-binding ability of HY5 to immobilize and purify the fusion protein on the microplate.

2. Materials

2.1. DBtag Protein Production

1. PCR thermocycler MP (Takarabio Inc., Otsu, Japan).
2. ExTaq DNA polymerase (Takarabio Inc.).
3. pEU-DBtag (accession no. AB369281) or Arabidopsis *HY5* gene (GenBANK accession no. NM_121164).
4. cDNA for synthesized protein.
5. Oligonucleotide primers.
6. Exonuclease I (1 U/10 μL reaction mixture, GE Healthcare, Little Chalfont, UK).
7. PCR product purification kit (Gel-M®Extraction, Viogene, Shijr, Taipei).
8. 5× Transcription buffer (TB): 400 mM HEPES-KOH, pH 7.8, 80 mM magnesium acetate, 10 mM spermidine, and 50 mM DTT.
9. Nucleotide tri-phosphates (NTPs) mix: a solution containing 25 mM each of ATP, GTP, CTP, and UTP.
10. SP6 RNA polymerase (80 units/μL, Promega; Madison, WI).
11. RNasin (80 units/μL, Promega; Madison, WI).
12. Microcon (YM-50; Millipore, Bedford, USA).

13. 10 mg/mL creatine kinase (Roche Diagnostics K. K.).
14. 4× Translational substrate buffer (TSB): 120 mM HEPES-KOH, pH 7.8, 400 mM potassium acetate, 10.8 mM magnesium acetate, 1.6 mM spermidine, 16 mM DTT, 1.2 mM amino acid mix, 4.8 mM ATP, 1 mM GTP, and 64 mM creatine phosphate. Or, 4× SUB-AMIX® (CellFree Sciences Co., Ltd., Matsuyama, Japan).
15. 1× TSB: 30 mM HEPES-KOH, pH 7.8, 100 mM potassium acetate, 2.7 mM magnesium acetate, 0.4 mM spermidine, 4 mM DTT, 0.3 mM amino acid mix, 1.2 mM ATP, 0.25 mM GTP, and 16 mM creatine phosphate. Or, 1× SUB-AMIX® (CellFree Sciences Co., Ltd.).
16. Wheat embryo extract (240 OD/mL, described in Chapter 3) or WEPRO®1240 (CellFree Sciences Co., Ltd.).
17. *Escherichia coli* biotin protein ligase (BirA, Genbank Accession no. NP_312927).
18. Biotin (Nakalai Tesque, Inc., Kyoto, Japan).

2.2. Protein Microarray Using Garose/DNA Microplate

1. Agarose (SeaKem Gold, Takarabio, Inc.).
2. Salmon sperm DNA (Sigma-Aldrich Corp, MO).
3. 1× TMD buffer: 20 mM Tris–HCl at pH 7.8, 2 mM $MgCl_2$, and 1 mM DTT.
4. Slide glass (Asahi glass, Japan).
5. Lab-Tek II Chamber slide (one-well, Nalge Nunc International Co., Naperville, IL).
6. Pin-type spotter like MultiSPRinter™ spotter (Toyobo Bio Instruments, Tsuruga, Japan) or comparable product.
7. Wash buffer: 20 mM Tris–HCl at pH 7.8, 200 mM NaCl, 2 mM $MgCl_2$, and 1 mM DTT.
8. Tupperware box.

2.3. Functional Protein Analysis Using the Protein Microarray

1. cDNAs.
2. 1× PBS buffer: 137 mM Nacl, 2.7 mM Kcl, 10 mM Na_2HPO_4, 1.8 mM KH_2PO_4, pH 7.4.
3. Kination solution: 50 mM Tris–HCl at pH 7.8, 100 mM NaCl, 10 mM $MgCl_2$, and 0.1 mM DTT, 10,000 Ci/μl [γ-^{32}P]-ATP, 0.05% DMSO (plus protein kinase inhibitor for inhibitor solution, if need be).
4. Caspase-3 solution: 20 mM Tris–HCl at pH 7.8, 200 mM NaCl, 2 mM $MgCl_2$, 1 mM DTT, and 17.4 ng/μL caspase 3 (human, Sigma-Aldrich Corp)].
5. 10μg/ml Alexa488-streptavidin (STA) (Invitrogen Corp., Carlsbad, CA).

6. Typhoon 9400 imaging system (GE Healthcare, Little Chalfont, UK) or comparable product.

3. Methods

3.1. Construction of DNA Template for DBtagged Protein Production

Arabidopsis *HY5* gene was inserted into pEU vector (4) as pEU-DBtag (Fig. 7.1a). The DBtag fragment (accession no. AB369281) was isolated (Subheading 3.1.1.) and fused on N-terminal of purpose gene by split-PCR (Subheading 3.1.2.). We have optimized a PCR-based linear template DNA generation by designing a set of universal primers for fusions of SP6 promoter and translational enhancer (E02) (9). For production of biotinylated protein, biotin ligation site (amino acid sequence: GLNDIFEAQKIEWHE)

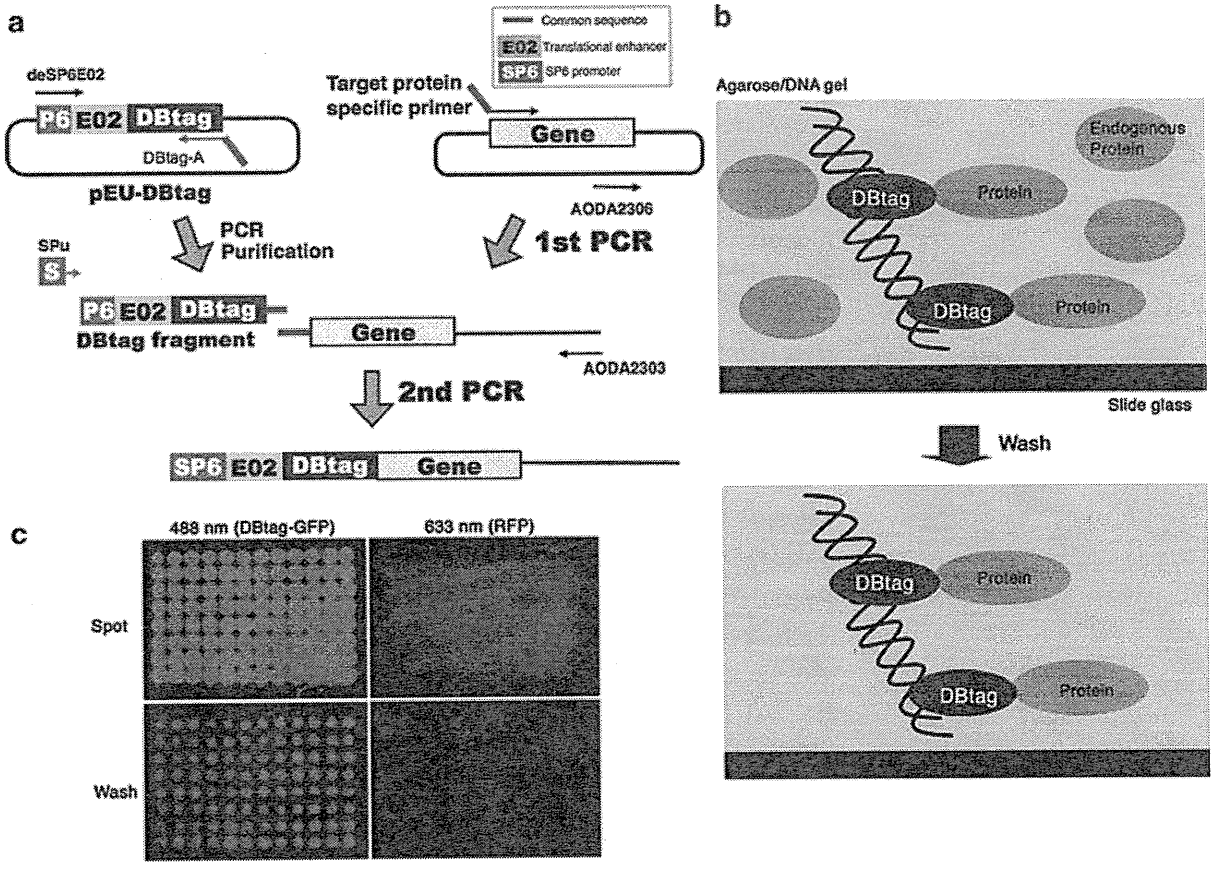

Fig. 7.1. (**a**) Scheme for DBtag-fusion method by the "split-primer" PCR. The DBtag fragment includes partial SP6 promoter. DNA amplification by SPu primer makes full-length SP6 promoter. (**b**) Schematic showing immobilized DBtag-fusion proteins on the microplate before and after washing. (**c**) DBtag-GFP and RFP (untagged) were mixed together and the mixture was spotted on the microplate. The DBtag-GFP was immobilized on the microplate, while the RFP was washed out and no RFP fluorescence was observed. Reproduced from ref. (7) with permission.